Paleotsunami deposits along the coast of Egypt correlate with historical earthquake records of eastern Mediterranean

Asem Salama, (1, 2, *), Mustapha Meghraoui (1**), Mohamed El Gabry (2, *), Said Maouche (3, *), Hesham Moussa Hussein (2, *), and Ibrahim Korrat (4)

[1.] EOST-IPGS - CNRS - UMR 7516, 5 rue René Descartes, Strasbourg, France
[2.] NRIAG, 11421 Helwan, Egypt
[3.] CRAAG, Bouzareah, Algeria
[4.] Dept. of Seismology, Mansoura University, Mansoura, Egypt

* Also at *North Africa Group for Earthquake and Tsunami Studies (NAGET), Ne t40/OEA ICTP, Italy*

***Corresponding author*

Submitted to Natural Hazards and Earth System Sciences (*NHESS*)

March 2018

Abstract.

We study the sedimentary record of past tsunamis along the coastal area west of Alexandria (NW Egypt) taking into account the occurrence of major historical earthquakes in the eastern Mediterranean. The two selected sites at Kefr Saber (~32-km west of Marsa-Matrouh city) and ~10 km northwest of El Alamein village are coastal lagoons protected by 2 to 20-m-high dunes parallel to the shoreline. Field data were collected by: 1) Coastal geomorphology along estuaries, wedge-protected and dune-protected lagoons, and 2) identification of paleotsunamis deposits and their spatial distribution using five trenches (1.5-m-depth) at Kefr Saber and twelve cores (1 to 2.5-m-depth) at El Alamein. Detailed logging of sedimentary sections were analysed using X rays, grain size and sorting, total organic and inorganic matter, bulk mineralogy, magnetic susceptibility and radiocarbon dating necessary for the identification of past tsunamis records. Generally of low energy, the stratigraphic succession made of marine and alluvial deposits includes intercalated high-energy deposits made of mixed fine and coarse sand with broken shells, interpreted as catastrophic layers correlated with tsunami deposits. Although the radiocarbon dating of 46 samples consist in mixed old (> 13000 year BP) and young (< 5500 year BP), dated charcoal and shell in sedimentary units allow the correlation with the 24 June 1870 (Mw 7.5), 8 August 1303 (Mw ~8) and 21 July 365 (Mw 8 – 8.5) large tsunamigenic earthquakes that caused inundations in Alexandria and northern Egyptian shoreline. Our results point out the size and recurrence of past tsunamis and the potential for tsunami hazard over the Egyptian coastline and the eastern Mediterranean regions.

1. Introduction:

Egypt has a well-documented historical catalogue of earthquakes and tsunamis recorded in ancient texts and manuscripts. Original documents and archives from past civilizations are considered as the principal sources of macroseismic data for major historical earthquakes and tsunamis (Poirier and Taher, 1980; Maamoun et al., 1984; Ambraseys et al., 1994, 2009; Guidoboni et al., 1994, 2005; Soloviev et al. 2000, Tinti et al., 2001). The catalogue of Ambraseys et al., 2009 reports that coastal cities of northern Egypt have experienced repeated tsunamis inundations with severe damage in the past. While historical earthquakes and tsunamis are well documented, it appears that there is a lack of holistic investigations for tsunami deposits along the Mediterranean coastlines. The geomorphology along the Mediterranean coastline of northern Egypt with low-level topography (Hassouba, 1995), dunes and lagoons constitutes an ideal natural environment for the geological record of past tsunamis.

The Eastern Mediterranean region experienced major earthquakes (with Mw > 7.5) mainly along the Hellenic subduction zone due to the convergence between the Eurasian and African plates (Fig. 1; Ambraseys et al., 1994, Taymaz et al., 2004). Major historical tsunamis in the eastern Mediterranean region that affected northern Egypt are triggered by large earthquakes (Papadopoulos et al., 2014) but the possibility of landslide tsunami associated with local earthquakes (El-Sayed et al., 2004) may also exist. Yalciner et al. (2014) estimated that up to 500 km^3 landslide volume, with wave height ranging from 0.4 to 4 m, might have taken place offshore the Nile Delta. However, the effects of landslide tsunami are limited to the nearby coastline as shown by the recent examples of landslide tsunamis in the Mediterranean (Tinti et al., 2005).

Tsunami research of the past 20 years has led to the discovery of coastal tsunami sedimentary records dating back to thousands of years. Among the early studies, the evidence of more than 6 soil levels buried below tsunami deposits in the past 7000 years were found at Puget Sound coastline of Washington state (Atwater, 1987). Nanayama et al. (2003) recognized major tsunamis due to extensive coastal inundation along the eastern coast of Hokkaido (northern Japan); the repeated sand sheet layers several kilometres inland evidenced a 500-year tsunami cycle in the period between 2000 and 7000 years BP. Following the 2004 Sumatra earthquake (Mw 9.1) and tsunami, Malik et al. (2015) identified in trenches three historical tsunamis during the past 1000 years along the coast of South Andaman Island (India). In the Mediterranean, De Martini et al. (2012) identified two tsunamis deposits during the first millennium BC and another one in 650-770 AD and estimated 385 year average recurrence interval for strong tsunamis along the eastern coast of Sicily (Italy).

In this paper, we investigate the paleotsunami deposits in the northern coast of Egypt and their correlation with the historical tsunami catalogue of the Eastern Mediterranean. Using coastal geomorphology with trenching and coring, we examine the geological evidence of tsunami deposits using geochemical analysis, magnetic susceptibility and radiocarbon dating to identify the tsunamis records. The Bayesian simulation (Oxcal 4.2; Bronk-Ramsey, 2013) is applied to the radiocarbon results and stratigraphic succession of coastal deposits in order to generate a precise paleochronology of tsunami events. Finally, we discuss the evidence of paleotsunamis and their dating in comparison with the major historical tsunamigenic earthquakes of the Hellenic and Cyprus subduction zones.

2. Major historical tsunamis of the Mediterranean coast of Egypt

The tsunami catalogue of Egypt cites the work of Guidoboni et al. (1994, 2005) and Ambraseys (2009) that report several large historical tsunamigenic earthquakes with severe damage in the eastern Mediterranean regions (Table 1). Among these events, the tsunamis of

21 July 365, 8 August 1303 and 24 June 1870 inundated the harbour of Alexandria city as well as the Mediterranean coast of Egypt.

Early in the morning of 21 July 365, an earthquake with estimated magnitude ~Mw 8-8.5 located offshore West of Crete generated a major tsunami that affected the eastern Mediterranean coastal regions (Ambraseys et al., 1994). A contemporaneous account from the Roman historian Ammianus Marcellinus (~~born 325 – 330, died c. 391 – 400;~~ Guidoboni et al., 1994) reported the sudden retreat of the sea and the occurrence of a “gigantic” wave inland with inundation and damage to the Alexandria harbour and city where ships were lifted inland on house roofs; the estimated wave height of this tsunami was calculated by Hamouda (2009) to be larger than 8 m in Alexandria. The seismic source of this earthquake is located in ~~west~~ Crete, according to archeological and historical damage distribution, combined with coastal uplift measurements and modelling (Fig. 1; Guidoboni et al., 1994; Stiros, 2001; Shaw et al., 2008 and Ambraseys, 2009).

On 8 August 1303 a major earthquake with magnitude ~Mw 8 located in between Crete and Rhodos islands generated a tsunami that greatly damaged the coastal cities of the eastern Mediterranean (Guidoboni and Comastri, 2005; Ambraseys, 2009). Abu-El Fida (1907) reported ~~in 1329~~ that the Alexandria city and Nile delta were flooded and many houses were damaged in Cairo and northern Egypt. In Alexandria, part of the city walls collapsed, the famous lighthouse was destroyed and some ships were torn apart carried up inland due to the tsunami waves (Abu-El Fida, 1907). In a recent synthesis of major seismic sources, Papadopoulos et al. (2014) locate the 1303 earthquake in between Crete and Rhodos Islands of the Hellenic subduction zone (Fig. 1).

On 24 June 1870, a large earthquake affected many places of the eastern Mediterranean region and was felt in Alexandria at around 18 h with no damage in the city but with slight damage in Cairo (Ambraseys, 2009). In Alexandria coastline and Nile Delta, the sea ~~wave~~ flooded the ~~quays~~ of ports and inland fields (Coumbary, 1870). The seismic source location of this earthquake at the eastern edge of Crete is inferred from the damage in Heraklion and ~~felt~~ shaking around the east Mediterranean (Fig. 1; Schmidt, J.F., 1879; Jusseret and Sintubin, 2017).

Among these three reported earthquakes, it appears that the AD 365 and AD 1303 that can be classified as very large earthquakes (with Mw ≥ 8; Stiros, 2001; Shaw et al., 2008; Hamouda, 2006, 2009) generated major tsunamis with basin-wide impacts, while the 1870 earthquake may be of a lower magnitude (Mw ~7 – 7.5; Ben Menahem et al., 1991; Soloviev, 2000). Several studies of the 21 July 365 and 8 August 1303 historical earthquakes refer to tsunami waves with inundation in Alexandria and coastlines of northern Egypt, and therefore with the potential of tsunami records in the sedimentary deposits. However, there have been some debates on the 1870 event concerning its location, size and the possibility of tsunami waves, but several authors (Soloviev et al., 2000; Ben Menahem et al., 1979; Salamon et al., 2007; Papadopoulos et al., 2010; and Maramai et al., 2014) support the tsunami generation by 1870 earthquake.

3. Coastal geomorphology and site selection ~~of~~ paleotsunami record~~s~~

The northwest Mediterranean coast of Egypt forms the northern extremity of the Marmarica plateau which is a Miocene homoclinal limestone that extends west of Alexandria for about 500 km, acting as a major catchment area feeding the drainage system (Fig. 1). The plateau runs from the Qattara Depression southward to the piedmont plain northward with various elevations reaching ~100 m at Marsa Matrouh escarpment. The geomorphological landform of the study area is characterized by a 60-m-high northern plateau that includes ridges, sand dunes, lagoons, and rocky plains within a 20-km-wide strip along the coastline

(Fig. 1). The rocky Pleistocene limestone ridges include a veneer of carbonate sand that are mostly composed of oolitic grains (Frihy et al., 2010).

Coastal dune-ridges protect inner lagoons from the sea and constitute outstanding landform features at several locations parallel to the shoreline (Figs 2 and 3). These dunes are weathered where the rocky headlands outcrop (Abbas et al., 2008). The 2 to 20-m-high coastal beach-dune ridge mainly composed of oolitic and biogenic calcareous sand separates coastal lagoons and *sabkhas* (salt lake) from the sea. The beach-dune ridge is developed along the receding Quaternary shorelines and embayment of the Mediterranean Sea (Hassouba, 1995). The lagoons with flat depressions separated from the sea by the coastal dunes (with different heights and sometimes with seawater outlets) are designated sites for the record of past tsunami deposits.

The accumulation of large boulders (Shah-Hosseini et al., 2016) near the selected sites is considered as a possible witness of past tsunami events. However, the boulders along the coastlines may either results from storms (Hall et al. 2006; Spiske et al. 2008) or tsunami waves (Goff et al. 2006; 2009; Morhange et al. 2006). The majority of boulders observed near our investigated sites shows imbricated positions of large blocks directed toward south, a situation comparable to the tsunamigenic boulders studied along the Algerian coastline (Maouche et al. 2009).

The discrimination between storm and tsunami deposits is a challenge in the Mediterranean regions (Maouche et al., 2009; Marriner et al., 2017). However, the tsunami stratigraphic record is less frequent (according to Tinti et al., 2001) and often presents a specific sedimentary signature with mixed deposits that include: 1) The basal contact of tsunami layer is extremely sharp with loading structures where layers contain organic rich mud and vegetation (Matsumoto et al., 2008; Switzer and Jones 2008); 2) the presence of rip up clasts that also suggest considerable erosion of lagoon deposits usually associated with tsunami deposits (Szezucinski et al 2006); 3) The tsunami deposits tend to be much more poorly sorted than storm deposits (Paris et al., 2007); 4) the large number of mixed and often broken bivalve and shells that occupy large vertical and lateral stratigraphic positions (Donato et al., 2008); 5) the tsunami deposits tend to have laminations and or cross bedding due to landward or seaward current (Tuttle et al., 2004); 6) the particle sizes of tsunami sediments fine landward from the shores (Srinivasalu et al., 2009); 7) the grain size are often bimodal particles size than the storm which tend to have unimodal particle size (Paris et al., 2007); 8) The increase of concentrations of Na, S, Cl, Mg with the presence of heavy minerals in tsunami deposits (Szczucinski et al., 2006; Babu et al., 2007); and 9) The low peak value of magnetic susceptibility linked to the amount of sand originated from the littoral dunes and reworked mixed sediments from tsunami waves (Font et al., 2010).

The local geomorphological and topographic settings contribute to the site selection for paleotsunami investigations. Our site selection for trenching and coring took into account the accessibility to dry lagoons (during summer season) in areas with no urbanization or artificially reworked soil. Suitable sites for trenching and coring are located in areas protected from the sea by ~~the rather~~ low (~2-m-high) sand dune topography that allows tsunami waves and related material to deposit into the lagoon. Two ~200 km apart sites of seasonal dry lagoons have met the selection criteria for paleotsunami investigation (Figs. 1 and 2): 1) Kefr Saber located at ~32-km west of Marsa-Matrouh city, and 2) El Alamein site at ~10 km northwest of El Alamein city and ~150 km west of Alexandria. Five trenches were dug at Kefr Saber (Fig 2a), and 12 cores were performed at the El Alamein site (Fig 2b).

4. ~~Used~~ methods for paleotsunami investigations

The trench size is ~2 x 1 meter with ~1.5-m-depth depending on the water table reach; all trench walls exposed fine-grained sedimentary layers ~~and~~ were logged in details. The maximum core depth is ~2.6 m and their distribution in the lagoons was planned to occupy an area from the depression (depo-centre) to the edge close to the outlet of seawater in order to observe any thickness variation of tsunami layers.

The core tubes were split in half lengthwise, photographed using both normal and ultra-violet lightning accompanied by detail description of textures and sedimentary structures. An X-ray scanning was performed immediately after core opening and all cores were sent to the laboratory of the National Institute of Geophysics and Astronomy (NRIAG, Cairo) for sampling and further analysis. The magnetic susceptibility measurements were operated along cores and samples were collected for radiocarbon dating, physical, chemical and organic matter analyses.

The magnetic susceptibility was measured for cores at the NRIAG Rock Magnetism laboratory then corrected against air by using Bartington compatible software. 120 samples were collected from cores then analysed for grain size analysis; X-ray diffraction using Philips PW 1730. The total organic and inorganic measurements were carried out at the laboratory of Central Metallurgical Research & Development Institute (CMRDI at Eltebbin, Egypt). Statistics of the grain-size distribution were calculated using Folk equations (1968) to obtain mean size and sorting of the sediments along the cores.

The Radiocarbon dating of samples are carried out in three laboratories (Poznan laboratory - Poland, CIRAM in Bordeaux, France and Beta Analytical laboratory, USA) to ensure coherency and quality of results (see Tables 2 a and b). The collected samples are made of charcoal, bones, gastropods, shells and organic matter. The radiocarbon dating results of samples are subsequently corrected using a recent calibration curve (Reimer et al., 2013) and the Oxcal software (Bronk-Ramsay, 2009) for the probability density function with 2σ uncertainty for each dated sample. In addition, from a succession of calibrated dates, a Bayesian analysis provides the simulated age in probability density function of a catastrophic event. The simulated age allows the correlation between the tsunami layer deposits, the related isotopic chronology and the historical tsunami events in catalogues.

5. Description of trenches and cores sedimentary layers

The selected sites revealed a succession of sedimentary units typical of lagoon deposits with fine strata made of a mix of fine gravel, sand, silt and clay (Salama, 2017). At both Kefr Saber and El Alamein sites, trenches and cores present comparable soft sediment content and stratigraphy. The variation of sediments content in the different cores is due to the distance from the shore and to the core location in the lagoons with regard to dunes heights. A detailed description of the trenches and cores at both Kefr Saber and El Alamein sites is presented here below:

5. 1. Kefr Saber site: Trenches P1, P2, P3 and P4 are 20 to 40 m distance, have quite similar sedimentary succession with fine-grained mostly alluvial deposits made of sandy-silty layers with mixed coarse and white fine sand that contains broken shells of marine origin (Fig. 3 and trench logs in supplemental material S1). A conspicuous layer of white mixed sand, gravel and broken shells with variable 2 to 15 cm thicknesses is found at 30 – 50 cm depth in P1, P2, P3; its thickness decreases landward to 1 cm in P4 (see supplemental material S1 a, b, c, d, e). Trench P5 which is close to the dunes and shoreline shows a succession of coarse and fine sand, and 30 to 40 cm thick mixed with pebbles which, as observed in other trenches, are fining inland. According to Goff et al., 2006, the high energy fining inland sedimentary sequence is related to tsunami deposits rather than storm deposits. The white mixed sand with broke shells characterized by high-energy sedimentary deposits is interpreted as of tsunami origin.

The mixed radiocarbon dating of samples in trenches is an issue at Kefr Saber. Two charcoal samples collected in Trench P1 at 35 cm and 53 cm depth display modern age (younger than 1650 AD) and 39000-38250 BC, respectively. In Trench P2, two other charcoal samples collected at 73 cm and 100 cm depth and both below the tsunami layer labelled 1 (Fig. S1-b) indicate 50 - 70 AD and 5300-5070 BC, respectively (see also Table 2a). In Trench P4, four collected charcoal samples at 15 cm, 25 cm, 40 cm and 61 cm depth reveal modern ages (younger than 1650 AD). A fifth charcoal sample located at 60 cm depth provides 17200- 15900 BC. In Trench P5, four charcoal samples are collected with the uppermost sample located at 12 cm depth is dated at 360-50 BC, the second sample at 17 cm depth show 30- 180 AD, the third, and fourth charcoal samples found at 33 cm and 37 cm depth are dated at 350 - 1050 BC and 2400-4000BC, respectively. The mixing between old (older than 7000 years BP) and relatively young ages (younger than 2000 years BP) denotes of the deposit of reworked layers within an environment of young sedimentation in lagoon.

Results: Although the sedimentary deposits in trenches at Kefr Saber indicate mixed and reworked sedimentation, the well identified coarse and fine white sand layer with broken shells of marine origin located ~ 30 - 73 cm depth in all trenches P1 to P4 suggests a single homogeneous sedimentary unit of relatively young age deposited in the lagoon. Considering that the stratigraphic succession and related chronology are comparable in all trenches dug in the same lagoon, we selected the radiocarbon dates younger than 2000 year BP that bracket the white sandy layer unit (i.e., samples TSU P5 S4 and S5, TSU P3 S1 and S3 that predate the unit, and sample TSU P3 S2 that postdates the unit). The Oxcal dating simulation provides the 137 – 422 AD bracket of the white sandy layer unit that may be correlated with the tsunami deposits of the 21 July 365 earthquake (Fig. 4).

North of the trench sites at Kefr Saber, the dating of shells (Dendropoma) of a sample collected in a large boulder provide a radiocarbon calibrated date of 940-1446 AD. The dating of Dendropoma collected in a boulder often marks the catastrophic coastal environmental change with displaced large boulders from an intertidal to shoreline position due to a tsunami event (Goff et al., 2012). The Dendropoma sample age at Kefr Saber may correlate with the 8 August 1303 earthquake and tsunami event that dragged large boulders on the shoreline in agreement with the results of Shah-Hosseini et al. (2016). However, we could not identify the 1303 event in the trenches dug in the nearby lagoon at Kefr Saber.

5. 2. El Alamein site*:* The 12 cores extend between 1 m and 2.6 m depth and except for cores 1 and 9 which are shown in Figures 5 a and b, the detailed stratigraphic logs and related measurements are presented in the supplemental material S2. In a previous reconnaissance field investigation, a coarse and fine white sand layer was identified ~ 30 cm depth in a test pit. Two charcoal samples El Al sa1 and El Al sa2 collected at 25 cm and 56 cm depth give 1680-1908 AD and 1661-1931 AD ages, respectively. The description of cores is as following:

Core 1: This core is located at ~166 m from the shoreline (Fig. 2 b), east of the study area behind the sand dunes and near the outlet of the seawater. The core depth reached ~2.14 m and the stratigraphic section includes 3 tsunami layers recognized as following (Fig. 5 a section 1 and its continuation at depth in Fig. S2-1):

The first layer is at ~12.5 cm depth with ~34.5 thick, brown clay sediments with poor sorting, fine grain sediments, with high peak in magnetic susceptibility, rich in organic matter, and X-ray image reflects clear lamination. The second layer which is located at ~70 cm depth has ~5 cm thickness, characterized by highly broken shells fragments with the extremely bad sorting of sediments granulometry. The third layer at ~75 m depth is ~22 cm thick, made of pale yellow sand with bad sorting of sediments size, and a peak in magnetic susceptibility. The chemical analysis shows the presence of gypsum and minor goethite, and X-ray scanning shows some turbiditic structures. A fourth tsunami layer is identified at 158 cm (see Fig. S2-1; section 2). It is characterized by pale brown silty clay, with broken shells fragments and extremely poor sorting, and with a high peak of magnetic susceptibility.

Two samples were collected for radiocarbon dating from core 1. The first and uppermost sample is a charcoal fragment at 40 cm depth located within a layer of catastrophic mixed sedimentary unit characterized by bad sorting, highly broken shells fragments and the peak of magnetic susceptibility. We interpret this layer as of tsunami origin and although its stratigraphy is located close to the surface, the mixed and reworked sedimentation explains the obtained old age 13985- 14415 BC (Table 2b). The second sample is a rodent bone at 50 cm depth and provides 403-603 AD calibrated age that postdate a catastrophic layer made of white sandy layer with broken shells. This catastrophic layer may correlate well with the 365 AD major earthquake of the eastern Mediterranean.

Core 2: As shown in core 2 is ~90 cm deep located south of core 1 at ~264 m from the shoreline (Fig. 2 b, Fig. S2 – 2). Two tsunami layers are identified. The first tsunami layer is ~12 cm thick brown clay sediments at ~13 cm depth, mixed with gravel and sand. The layer is rich in organic matter (> 1), with a small peak of magnetic susceptibility and where the geochemical analysis shows a minor component of goethite. The second layer at ~50 cm depth is ~15 cm thick, made of mixed yellow sand with silty-clay pockets, broken shells fragments, poor sorting and with peak magnetic susceptibility. It is rich in organic matter comparing to the other layer, and the geochemical analysis shows minor component of halite.

Several samples were collected below and above the tsunami layers but, unfortunately, their content did not deliver enough carbon for dating. The two shells (gastropod) samples collected at 75 cm and 77 cm depth (well below the lowermost tsunami layer, Fig.S2-2) have calibrated dates 32971-34681 and 34362-36931 BC, respectively (Table 2b). These obtained ages may well be due to a mixed and/or reworked sedimentation.

Core 3: This core is located at 270 m from the shoreline and the outlet of sea water has revealed three tsunami layers (Fig. 2b and Fig. S2 – 3). The first tsunami layer is at ~25 cm depth and corresponds to 26 cm thick pale brown clay characterized by broken shells fragments and sediments rich in organic matter. The second layer at ~70 cm depth is 17.5 cm thick characterized by white sand laminated at the top with a peak of magnetic susceptibility near zero value, and with high organic matter > 2. The third tsunami layer at 106 cm depth is 32 cm thick, characterized by yellow sand with minor illite and broken shells fragments.

Two shell samples were collected for dating at 37 cm and 45 cm depth and show calibrated dates 43618 BC and 34218-37224 BC respectively (Fig.S2-3 and Table 2b). These two samples are located within the stratigraphic tsunami layer 2 and may correspond to reworked sediments due to the high energy sedimentation during the catastrophic event.

Core 4: The core is located at 435 m from the shoreline and shows sedimentary units where we identify two tsunami layers with high magnetic susceptibility (Fig. S2 - 4). The first tsunami layer is the white sand at ~12.5 cm depth 7 cm thick with poorly sorted sediments, broken shells fragments with organic matter > 2. The second tsunami layer is a pale yellow sand at ~102 to 130 cm depth, characterized by broken shell fragments in a yellow sand with a minor amount of illite and gypsum.

One shell sample collected for dating at 37 cm depth provides a calibrated date 32887-34447 BC respectively (Table 2b). This sample located in the stratigraphic tsunami layer 1 apparently results from high energy reworked sedimentation during the catastrophic event (Fig. S2-4).

Core 5: This is the southernmost core in the El Alamein site, located at 490 m distance from the shoreline (Fig. 2 b; Fig. S2 - 5). The core reaches 73 cm depth and the sedimentary succession does not show any possible catastrophic sedimentary layer of tsunami origin. According to its content, core 5 may show the limit of inundation area with respect to at least the first and second tsunami layers.

Core 6: This core is located south of the sand dunes at 320 m from the shoreline (Fig. 2 b). It is characterized by three tsunami layers (Fig. S2 - 6). The first tsunami layer is a ~24 cm thick pale yellow sand with broken shells fragments (between 5 and 26 cm depth) and poorly sorted sediments rich in organic matter (larger than 2.5). The second tsunami layer is ~18.5 cm thick at 50 - 75 cm depth characterized by yellow sand with mixed gastropods and bivalves, and a high value of magnetic susceptibility. The third tsunami layer at 130 cm depth is ~20 cm thick, rich in organic matter, characterized by white sand mixed with gravel and pebble and broken shells fragments.

Three samples were collected for dating in core 6. The first sample is a gastropod at ~45 cm depth and shows 35002-37441 BC calibrated date. The second and third samples are coral fragments at ~60 cm and ~80 cm depth that gave 42776-69225 BC and modern (younger than 1650AD) calibrated ages. The first sample is above the tsunami layer 2 while the second sample was within the stratigraphic tsunami layer 2 (Fig S2-7). These samples may result from mixed sedimentation and reworking due to high current waves transport of tsunamis.

Core 7: This core was located at 273 m from the shoreline (Fig. 2 b). It is characterized by sedimentary units that may include three tsunami layers within 120 cm core depth (Fig. S2 - 7). The first tsunami layer is a 6 cm thick brown sand with broken shell fragments at ~14 cm depth and a considerable amount of gypsum with a minor amount of Illite and goethite. It is rich with organic matter (> 2) of a swampy environment and the noticeable peak of magnetic susceptibility. The second tsunami layer at 50 cm depth is 20 cm thick, characterized by laminated pale brown clay mixed with gravel and pebbles at the bottom. The third tsunami layer is 15 cm thick at 115 cm depth characterized by white sand, bad sorting sediments with aminor amount of pyrite.

A single sample of shell fragment collected at 17 cm depth for radiocarbon dating within tsunami layer 1 provides 293-1113 BC.

Core 8: This core is located at 214 m from the shoreline (Fig. 2 b). Three tsunami layers are recognized (Fig. S2 - 8). The first tsunami layer is 16 cm thick pale silty clay at ~14 cm depth, rich in organic matter, with minor amount of goethite, characterized by highly broken shell fragments. The second layer is a 22 cm thick at ~52 cm depth, of pale yellow silty-clay with broken shells, characterized by a high peak of magnetic susceptibility and rich inorganic matter (>2.5). The third tsunami layer is 9 cm thick at ~128 cm depth, characterized by pale yellow sand with broken shells fragments and badly sorted angular gravel sediments. No samples were suitable for dating in this core.

Core 9: The core is located at 130 m from the shoreline. Three tsunami layers are recognized (Fig. 5 b; Fig. S2 - 9). The first tsunami layer is white sand at ~16 cm depth and 13 cm thick with ahigh content of organic matter and rips up clasts that appear in X-ray scanning characterized by highly broken shells fragments and rich in organic matter. The second layer at 67 cm depth is 22 cm thick characterized by white sand, with a peak of magnetic susceptibility, high content of organic matter larger than 5. The third tsunami layer at 139 cm depth is 14 cm thick characterized by broken shells fragments and white sand with highly angular sediments that reflect the ~~bad~~ granulometric sorting.

Two samples were collected for dating in core 9. The first sample is a gastropod shell located at 24 cm depth within the tsunami layer 1 ~~that~~ gives 1052-1888 BC calibrated age. The second sample at 55 cm depth is a bivalve (lamellibranch) located above the tsunami layer 2 dated at 40521-43169 BC calibrated age. These samples may have been transported and re-deposited due to high current waves of the tsunami events.

Core 10: The core is located at 245 m from the shoreline (Fig. 2 b). Three tsunami layers are recognized (Fig. S2 - 10). The first tsunami layer is 9 cm thick brown silty clay, at ~19 cm depth with broken shells fragments, rich in organic matter (> 4) and high peak of magnetic susceptibility; rip up clasts and laminations appear in X-ray scanning. The second layer 38 cm thick brown sand at 48 cm depth with broken fragments of shells, peak of magnetic susceptibility and high organic matter (> 1.5) at the bottom of the layer. The third tsunami layer is 28 cm thick pale yellow sand at 101 cm depth characterized by rich organic matter and sediments that reflect the bad sorting.

Two samples were collected for dating in core 10. The first sample located in the tsunami layer 1 is a shell fragment at 24 cm depth that gives 2623-3521 BC calibrated age. The second sample located in the tsunami layer 2 is a rodent bone at 70 cm depthshowing 41256-46581 BC calibrated age (see also Table 2b). Both samples may result from reworked sedimentary units due to high current waves of tsunami events.

Core 11: The core is located at 151 m from the shoreline (Fig. 2 b). Three tsunami layers are recognized (Fig.S2 - 11). The first tsunami layer is 10 cm thick white sand with broken shell fragments at ~19 cm depth; the layer also shows high magnetic susceptibility, rich organic matter (> 4) with a high percent of gypsum (>50%). The second layer is 9 cm thick white sand at 76 cm depth, with broken shell fragments, a high peak of magnetic susceptibility and organic matter larger than 1.5. The third tsunami layer is 21 cm thick grey silty sand, with broken shell fragments at 107 cm depth; ~~bad~~ sorting, high organic rich matter and a minor amount of Illite and gypsum.

Eight samples were collected for dating in core 11. The sedimentary units at 112 - 175 cm depth (core bottom) and related succession of ages between 3943 BC and 2475 BC (from shell gastropods and a charcoal fragment; see Table 2 b), may indicate a consistent dating of the tsunami layer 3. However, the first sample (gastropod shell) at ~20 cm depth that gives 3638-4328 BC, the second sample (broken shell) at 62 cm depth with an age at 17869 - 18741 BC, and the 33294 – 36120 BC and 2619 – 3386 BC out of sequence dating (Table 2 b) ~~indicate samples of transported and reworked shells and sediments probably due to high energy tsunami deposits.~~

Core 12: The core is located at 127 m from the shoreline (Fig 2 b). Three tsunami layers are recognized in section 1 and one tsunami layer in section 2 (Fig. S2 – 12 a, b). The first layer is ~7.5-cm-thick at ~19-cm-depth and is made of poorly sorted white sandy deposits, and highly broken gastropods and lamellibranch fossils. The layer is characterized by high values of organic matter and magnetic susceptibility. The second layer is ~13-cm-thick white sandy deposits intercalated with coarse brown sand at ~32.5-cm-depth, characterized by horizontal lamination, poor sorting sediments, rich in organic matter and high peak of magnetic susceptibility. The third layer is ~25-cm-thick grey sandy clay at 89-cm-depth, with laminations at the bottom of deposits, vertically aligned gastropods, broken shells fragments, rich in total organic matter and a high peak of magnetic susceptibility. A fourth tsunami layer of medium to fine pale yellow sand, with broken shells fragments, is identified in section 2 (Fig. S2 – 12 b) at 151 cm depth. It is characterized by ~~and~~ poor sorting, high peak of magnetic susceptibility, a large amount of organic matter (> 5.5) and high amount of gypsum.

Five samples were collected for dating in core 12. In core section 1, the first sample is a gastropod found at 44 cm depth that gives an age of 3367-3366 BC. The second sample is a shell found at 108 cm depth and shows an age of 3097-3950 BC (Table 2 b). The third sample is a gastropod found at 114 cm depth dated at 3331-4050 BC. The fourth and fifth samples in core section 2,sample are gastropod shells found at 117 cm and 135 cm depth with calibrated age 39560- 40811 BC and 3365-4071 BC, respectively (Table 2 b). The fourth sample is off sequence with respect to the other samples and may result from sediment transport and reworking due to high energy tsunami waves. The other samples are in sequence from 4071 to 2457 BC age, comparable to the sedimentary succession of core 11.

Results: The sedimentary deposits in the El Alamein lagoon also result from intercalated high-energy marine deposits into low energy marine and alluvial deposits with reworked sedimentation. A first observation in almost all cores is the existence of the white sand layer with broken shells of marine origin located ~ 10 cm to 75 cm depth in El Alamein site, and the identified three to four tsunami layers. The tsunami layers and their catastrophic content are identified in photography and X-rays, magnetic susceptibility, organic/mineral content and by the existence of mixed coarse and fine sand with broken marine shells. A main difficulty, however, is the age determination of the tsunami layers due to the mixed radiocarbon dates that can be ranged in old and young ages, between 50000 year BP - 13430 year BP, and 5065 year BP - 125 year BP, respectively, in all cores.

As the sedimentary units in the 1 m to 2.6 m depth cores result from young deposition processes with high-energy marine units intercalated into low energy marine and alluvial deposits, we consider the radiocarbon dating older than 13430 year BP as due to sedimentary units that include reworked material. Considering that the succession of 2.6 m uppermost deposits and related stratigraphic chronology are comparable in all cores in the El Alamein lagoon, we select the radiocarbon dates younger than 5500 year BP as representative of the recent sedimentary units that include tsunami layers. Using the radiocarbon dating of samples and related selected young ages, the sedimentary sequence of catastrophic layers and their ages obtained from the Bayesian simulation (Oxcal 4.2.4; Bronk-Ramsey, 2013) allow a correlation with the AD 365, AD 1303 and AD 1870 tsunamigenic earthquakes of the east Mediterranean Sea (Fig. 6). In addition, a fourth tsunami layer can be identified between 1126 BC and 1434 BC.

6. Summary of results from trenching and coring

The cores and trenches in both Kefr Saber and El Alamein sites show three main layers characterized by fine and coarse sand mixed with broken shell fragments that indicate the occurrence of high energy and catastrophic sedimentary deposits in the coastal lagoon environment (Figs. 2 a, b, and c, and Fig. 3). Although the two studied sites are ~200 km apart, a white sandy layer with broken shells is found in all trenches (see Fig. 3 and supplemental material S1 a, b, c, d, e) and cores (except for core 5, see Figs. 5 a and b, and supplemental material in Fig. S2 – 1 to 12). The recurrent white sandy deposits in trenches and cores are well visible coarse sand units mixed with gravel and broken shells that become fine landward (see trench P4, Fig. 3) or disappear when distant from the shore (core 5, Fig. S2 – 5). All these signatures with only three layers in the ~ 2 m thick sedimentary units indicate that this layer suggests tsunami deposits rather than storm.

In most cores (Figures. 5 a and b, and supplemental material Fig. S2 – (1 - 12), the first tsunami layer is ~7.5-cm-thick at ~19 cm-depth and is made of poorly sorted white sandy deposits with broken gastropods and lamellibranch (shell) fossils. This layer is characterized by bi-modal grain size distribution with high value of organic matter and peak of magnetic susceptibility with a rich content in carbonates and quartz. The presence of goethite and pyrite heavy minerals was found in the cores at the base of layer 1, which contains rip up clasts from underlying sediments. The second layer is ~13-cm-thick at ~32.5-cm-depth characterized by white sandy deposits intercalated with coarse brown sand horizontal lamination, very poor sorting of sediments, rich in organic matter and with a high peak of magnetic susceptibility. The pebbles also are found at the base of this layer which reflects a loading structure. A considerable amount of heavy minerals like Goethite and Pyrite can be found in this layer. The third layer is ~25-cm-thick at ~89-cm-depth is made of grey sandy clay, with a high peak of magnetic susceptibility, laminations at the bottom of deposits, vertically aligned gastropods, broken shells fragments, and rich in total organic matter. In all three layers, the poorly sorted sediments and organic content greater than 5 mark the high energy deposits and tsunami records (Folk, 1968). All these characteristics at the El Alamein site lead us to interpret the three sedimentary layers as tsunami deposits.

In a synthesis of all dated units in trenches and cores in Figures 4 and 6, the sedimentary succession of low energy marine and alluvial deposits intercalated with high-energy deposits provides evidence for the identification of four tsunami deposits at Kefr Saber and El Alamein sites. In the case of Kefr Saber trenches, the dating of charcoal fragments allows the bracket of a tsunami event with a simulated age between AD 137 and AD 422, which includes the AD 365 western Crete earthquake (Figs. 4 and Table 2 a). The dating of sedimentary units at the El Alamein site turned out to be more complex due to the reworked sedimentation with significant mix of old (> 13000 year BP) and young ages (< 5500 year BP; Table 2 b). Using the latter ages, the radiocarbon dating (including the Oxcal Bayesian analysis) of shells, bone and charcoals fragments at El Alamein site (Fig. 6) result in a sequence of ages that allow the bracket of an event W between 1434 BC and 1126 BC, and event X between AD 48 and AD 715, and event Y between AD 1168 and AD 1689, and an event Z between AD 1805 and AD 1935 (Figure 6). The three most recent simulated dates of tsunami events X, Y and Z correlate with the seismogenic tsunamis of AD 365, AD 1303 and AD 1870 reported in catalogues (Table 1).

Discussions and Conclusions

The identification of tsunami deposits within the stratigraphic layers and results of radiocarbon dating allow the chronological simulation of the three most recent tsunami events (Figs. 4 and 5). The historical seismicity catalogue of the Eastern Mediterranean reported two significant tsunamigenic seismic events of the Hellenic subduction zone that affected the Mediterranean coast of Egypt: 1) The 21 July 365 earthquake (Mw 8.3 – 8.5; Stiros and Drakos, 2006; Shaw et al., 2008), 2) the 8 August 1303 earthquake (Mw 7.8 – 8.0; Abu Al Fida, 1907; Ambraseys, 2009). A third tsunami event is also reported during the 24 June 1870 earthquake (Mw 7 - 7.5), but despite some debates on its occurrence, the inundation of the

Alexandria harbour leaves no alternative on the tsunami waves on the Egyptian coastline (see section 2). Hence, the dating of the three high energy sedimentary layers deposited along the Egyptian coastline at Kefr Saber and El Alamein sites correlate with the historically recorded seismogenic tsunamis of the Hellenic subduction zone.

In our study, the distinction of tsunami sedimentary records from storm deposits is based on: 1) The record of the small number (3 to 4) layers while storm deposits controlled by seasonal climatic catastrophic events should have been more frequent. 2) The existence of white sand sheet layers with broken shells at two sites (Kefer Saber and El Alamein) located ~200 km apart, bearing comparable age, structure and texture. 3) The existence of organic rich clasts in sand sheets of some cores (Shi et al., 1995; Gelfenbaum and Jaffe, 2003) which indicates a catastrophic event with sufficient energy to break and erode the coastal barrier made of the shoreline rocky headlands, organic sediments and coastal dunes before reaching the lagoons. 4) The bimodal distribution of the grain size of sandy sedimentary units that include a large proportion of broken shell comparable to that of tsunami deposits (Goff et al., 2001, 2004). 5) The correlation between the simulated ages of tsunami layers from the radiocarbon dating and the large historical tsunamigenic earthquakes of the eastern Mediterranean (Figs. 4 and 6). 6) The consistent depth of tsunami layers in cores of the El Alamein site (Fig. 7).

The lagoon sedimentary environment is a natural site of mixed and reworked marine and continental deposits that may explain the mixed radiocarbon dates (Tables 2 a and b). Indeed, by considering the mixed sedimentation of reworked deposits intercalated with new units, our selection of samples younger than 2000 year BP at Kefr Saber, and younger than 5500 year BP at El Alamein allowed us to distinguish between old and new isotopic dating and infer a consistent chronology of tsunami deposits. For instance at the El Alamein lagoon, the clear separation between old (50000 year BP to13430 year BP) and young (5065 year BP -

125 year BP) radiocarbon dating, with no intermediate dates of sedimentation, confirms the different origin and processes of deposition. The radiocarbon dating indicate that the white sand and coarse mixed layers represent deposits that may result from tsunamis events in 365, 1303 and 1870 (see Table 1). The first two events are large earthquakes with Mw≥8 with well documented tsunami waves in the historical sources. The evidence of the 365 tsunami seems to be widely recorded through widespread massive turbidities of the eastern Mediterranean region (Stanley et al., 2006; Polonia et al., 2016). The four main catastrophic layers in trenches and cores have physical and chemical characteristics that correlate with high energy environmental conditions of tsunami deposits. The four high magnetic susceptibility peaks of the four deposits also correlate with the high value of organic matter and carbonates.

The record of past tsunami deposits is favored by the low topography and platform geomorphology along the Egyptian Mediterranean coastline. The coastal environment with similar lagoons and dunes with large areas with relatively flat morphology allowed the deposits of catastrophic marine deposits intercalated within alluvial deposits. The lagoon shapes elongated along the shoreline at Kefr Saber and El Alamein sites explain the similarity between the sedimentary units and the tsunami deposits. The correlation between the core deposits at El Alamein and trench deposits at Kefr Saber are marked by the dating of tsunami deposits and the correspondence with the AD 365 earthquake. The succession of sudden high-energy deposits with low energy and slow sedimentation may include reworked units with a disturbance in their chronological succession. In comparison with the trench results of Kefr Saber, the sedimentary sequence from cores at El Alamein reveals mixed old and young dates likely due to the sedimentary environment with large lagoon and nearby topography with the supply of colluvial and alluvial deposits. Despite the richness of charcoal fragments, bones and shells in the sedimentary record, the reworking implies significant out of sequence dating and large uncertainties (see Table 2 b, among 30 samples 12 dated samples are > 30 ka).

Although the results of dated shells may be suspicious (due to the unclosed mineralogical system), their reliability is tested with the comparison of nearby radiocarbon dating.

The size of past tsunamis can be compared with the thickness of catastrophic sedimentary units in trenches of Kefr Saber and core units of the El Alamein site. It appears that the tsunami deposits of the AD 365 tsunamigenic earthquake have a larger thickness at Kefr Saber site than at the El Alamein site. In contrast, the thickness of sedimentary layers of the AD 1303 and AD 1870 are thicker at the El Alamein site. These observations can be justified by the proximity of the tsunamigenic source in western Crete of the AD 365 earthquake with respect to the Kefr Saber paleotsunami site, and the proximity of the AD 1303 and AD 1870 seismic sources in the east Hellenic Arc with regards to the El Alamein paleotsunami site. Our results on the identification of past tsunamis and their repetition along the coastlines in Egypt and North Africa are decisive for the tsunami wave propagation and hazard models in the East Mediterranean Sea (Salama, 2017).

Author contribution:

A. Salama and M. Meghraoui wrote the text manuscript; A. Salama did the analysis of trench and core deposits, and interpretation of tsunami events; M. Meghraoui, M. El Gabry, H. Hussein and I. Korrat did the earthquake data analysis and interpretation; all authors contributed to the field investigations.

Competing interests: The authors declare that they have no conflict of interest.

Supplement:

Supplementary data associated with this manuscript are:

- Figures S1 a, b,c, d and e of five trench logs of Kefr Saber site (trench P4 as Fig. 3).

- Figure S2 – 1 (section 2) to 10 of core descriptions of El Alamein site (cores 1 and 9 as Figs a and b).

Acknowledgments

We are grateful to Prof. Hatem Odah and NRIAG administration, and staff for their keen efforts and help during the development of this work. We are grateful to the North African Group for Earthquake and Tsunami studies (NAGET) and Drs. Assia Harbi, Adel Samy, Hany Hassen, Mohamed Maklad, Mohamed Sayed for support and discussions. We are grateful to the "*Centre d'Etudes Alexandrine"* for the lending of the COBRA instrument for coring. We address our special thanks to the Egyptian Armed Forces for issuing permissions and their support during field work. This research programme is conducted with the funding support of the ASTARTE EC project (Assessment, Strategy And Risk Reduction for Tsunamis in Europe - FP7-ENV2013 6.4-3, Grant 603839), the French-Egyptian IMHOTEP project, and the Academy of Scientific Research and Technology of Egypt.

References

Abbas, M.S., El-Morsy, M.H., Shahba, M.A. and Moursy, F.I.,: Ecological studies in coastal sand dune rangelands in the North-West of Egypt, Meeting of the Sub-network on Mediterranean Forage Resources of the FAO-CIHEAM Inter-regional Cooperative Research and Development Network on Pastures and Fodder Crops, Spai: , 389–393, 2008.

Abu al-Fida Ismail Ibn Hamwi (born 1273 – died 1331). : The Concise History of Humanity or Chronicles (in Arabic *'Tarikhu 'al-Mukhtasar fi Akhbar al-Bashar'* in 1329). Al-Husayniyah Press, Cairo, 2 volumes , 1112 p., 1907.

Ambraseys, N.N., Melville, C.P. and Adam, R.D.: The seismicity of Egypt, Arabia and Red Sea: A Historical Review, Cambridge University Press, 181 p., 1994.

Ambraseys, N.: Earthquakes in the Mediterranean and Middle East: A Multidisciplinary Study of Seismicity up to 1900, Cambridge University Press, 947 p., 2009.

Atwater, B.: Evidence for great holocene earthquakes along the outer coast of Washington state, Science, 236, 942 – 944, 1987.

Babu, N., Suresh Babu D.S. and Mohan Das P.N.: Impact of tsunami on texture and mineralogy of a major placer deposit in southwest coast of India, Environmental Geology 52, 71–80, 2007.

Ben Menahem, A.: Earthquake catalogue for the Middle East (92 B.C. to 1980 A.D.) Bollettino di Geofisica Teorica ed Applicata, 2I, 245-310, 1979.

Ben Menahem, A.: Four thousand years of seismicity along the Dead Sea rift, Journal of Geophysical Research, 96, 195–216, 1991.

Bronk-Ramsey, C.: Bayesian analysis of Radiocarbon, Radiocarbon, 51(1), 337–360, 2009.

Bronk-Ramsey, C., & Lee S.: Recent and Planned Developments of the Program OxCal, Radiocarbon, 55(2-3), 720-730, 2013.

Coumbary, A. : Sur le tremblement de terre du 24 juin 1870, Nouvelles Météorologiques Paris, 3, 200-201, 1870.

CMT catalogue: Centroid Moment Tensor catalogue of Harvard, http://www.seismology.harvard.edusearch.html, 2018.

De Martini, P.M., Barbano, M.S., Pantosti, D., Smedile, A., Pirrotta, C., Del Carlo, P., and Pinzi, S.: Geological evidence for paleotsunamis along eastern Sicily (Italy): An overview: Natural Hazards and Earth System Sciences, 12 (8), 2569–2580, 2012.

Donato, S.V., E.G. Reinhardt, J.I.Boyce, R. Rothaus & T. Vosmer.: Identifying tsunami deposits using bivalve shell taphonomy, Geology, 36 (3), 199-202, 2008.

El-Sayed, A., Korrat, I., and Hussein, H. M.: Seismicity and seismic hazard in Alexandria (Egypt) and its surroundings, Pure and Applied Geophysics, 161, 1003–1019, 2004.

Folk, R.L.: Petrology of sedimentary rocks, in Austin, Texas, HemphilPs Book Store, 182 p., 1968.

Font, E., C. Nascimento, Baptista M.A. & Silva P.F.: Identification of tsunami induced deposits using numerical modelling and rock magnetism techniques: A study case of the 1755 Lisbon tsunami in Algarve, Portugal, Physics of the Earth and Planets Interiors, 182, 187–198, 2010

Frihy, O.E., Deabes, E. a., and El Gindy, A. a.: Wave Climate and Nearshore Processes on the Mediterranean Coast of Egypt: Journal of Coastal Research, 261, 103–112, 2010.

Galanopoulos, A.G.: The seismic sea-wave of 9 Iouliou 1956, Praktika Academy Athens, 32, 90–101, 1957.

Goff, J., Chague-Goff, C., and Nichol, S.: Palaeotsunami deposits: A New Zealand perspective, Sedimentary Geology, 143 (1–6), 2001.

Goff, J. R., McFadgen, B. G., and Chagué-Goff, C.: Sedimentary differences between the 2002 Easter storm and the 15th century Okoropunga tsunami, southeastern North Island, New Zealand, Marine Geology, 204, 235–250, 2004.

Goff J, Dudley WC, de Maintenon MJ, Cain G, Coney JP.: The largest local tsunami in 20th century Hawaii, Marine Geology 226, 65–79, 2006

Goff, J.R., Lane, E., Arnold, J.: The tsunami geomorphology of coastal dunes, Natural Hazards Earth System Sciences, 9 (3), 847–854, 2009.

Goff, J., Chagué-Goff, C., Nichol, S., Jaffe, B., Dominey-Howes, D.: Progress in palaeotsunami research, Sedimentary Geology, 243, 70–88, 2012.

Guidoboni, E., Comastri, A. and Traina G.: Catalogue of Ancient Earthquakes in the Mediterranean area up to the 10th century, INGV-SGA, Bologna, 504 p., 1994.

Guidoboni, E., and A. Comastri : Catalogue of earthquakes and tsunamis in the Mediterranean area from the 11th to the 15th century, INGV-SGA, Bologna, 1037 p., 2005.

Gelfenbaum, G., and B. Jaffe .: Erosion and sedimentation from the 17 July, 1998 Papua New Guinea tsunami, Pure and Applied Geophysics, 160, 1969–1999, 2003.

Hassouba, A.B.H.: Quaternary Sediments from the Coastal Plain of Northwestern Egypt (from Alexandria to Elomayid), Carbonates and Evaporites, 10 (1), 8–44, 1995.

Hall AM, Hansom JD, Williams DM, and Jarvis J.: Distribution, geomorphology and lithofacies of cliff- top storm deposits: examples from the high-energy coasts of Scotland and Ireland. Marine Geology, 232, 131–155, 2006.

Hamouda, A.Z.: Numerical computations of 1303 tsunamigenic propagation towards Alexandria, Egyptian coast, Journal African Earth Science, 44, 37-44, 2006.

Hamouda, A.Z.: A reanalysis of the AD 365 tsunami impact along the Egyptian Mediterranean coast, Acta Geophysica, 58 (4), 687–704, 2009.

Jusseret, S. and Sintubin, M., Minoan Earthquakes: Breaking the Myth through Interdisciplinarity, Studies in Archaeological Sciences, Leuven University Press, 440 pp., 2017

Maamoun, M., Megahed, A. and Allam, A.: Seismicity of Egypt, NRIAG Bulletin, IV (B), 109–160, 1984.

Maramai, A., Brizuela, B., Graziani, L. : The Euro- Mediterranean tsunami catalogue. Annals of Geophysics, 57 (4), 1-26, 2014.

Marriner, N., Kaniewski, D., Morhange, C., Flaux, C., Giaime, M., Vacchi, M., and Goff, J.: Tsunamis in the geological record, Making waves with a cautionary tale from the Mediterranean, Science Advances, 1-12, 2017.

Malik, J.N., Banerjee, C., Khan, A., Johnson, F.C., Shishikura, M., Satake, K., and Singhvi, A.K.: Stratigraphic evidence for earthquakes and tsunamis on the west coast of South Andaman Island, India during the past 1000years, Tectonophysics, 661, 49–65, 2015.

Matsumoto, D., H. Naruse, S. Fujino, A.Surphawajruksakul, T., Jarupongsakul, N., Sakakura & M. Murayama : Truncated flame structures within a deposit of the Indian Ocean Tsunami: evidence of syn-sedimentary deformation, Sedimentology, 55, .1559-1570, 2008.

Maouche, S., Morhange, C. and Meghraoui, M.: Large boulder accumulation on the Algerian coast evidence tsunami events in the western Mediterranean, Marine Geology, 262 (1), 96-104, 2009.

Morhange, C., Marriner, N., Pirazzoli, P.A.: Evidence of Late-Holocene tsunami events from Lebanon, Z. Geomorphology, 46, 81–95, 2006.

Nanayama, F., Satake, K., Furukawa, R., Shimokawa, K., Atwater, B.F., Shigeno, K., and Yamaki, S.: Unusually large earthquakes inferred from tsunami deposits along the Kuril trench, Nature, 424 (6949), 660–663, 2003.

Paris, R., F., Lavigne, P.,Wassmer, and J.,Sartohadi : Coastal sedimentation associated with the December 26, 2004 tsunami in Lhok Nga, West Banda Aceh (Sumatra, Indonesia). Marine Geology, 238, 93–106, 2007.

Papadopoulos, G.A., E. Daskalaki, A. Fokaefs and N. Giraleas.: Tsunami hazard in the Eastern Mediterranean Sea: strong earthquakes and tsunamis in the West Hellenic Arc and Trench System, Journal Earthquake and Tsunami, 4 (3), 145-179, 2010.

Papadopoulos, G. A., Gràcia, E., Urgeles, R., Sallares, V., De Martini, P. M., Pantosti, D., González, M., Yalciner, A. C., Mascle, J., Sakellariou, D., et al.: Historical and pre-historical tsunamis in the Mediterranean and its connected seas: Geological signatures, generation mechanisms and coastal impacts, Marine Geology, 354, 81–109, 2014.

Polonia, A., Vaiani, S.C., de Lange, G.J.: Did the A.D. 365 Crete earthquake/tsunami trigger synchronous giant turbidity currents in the Mediterranean Sea?, Geology, 44, 191-194, 2016.

Poirier, J. P. and Taher, M.A.: Historical Seismicity in the near and Middle East, North Africa, and Spain from Arabic Documents (VIIth- XVIIIth Century). Bulletin Society Seismology American, 70 (6), 2185–2201, 1980.

Reimer PJ, and 24 co-authors.: Selection an treatment of data for radiocarbon calibration: an update to the International Calibration (IntCal) criteria, Radiocarbon, 55 (4), 1869-1887, 2013.

Salama, A.: Active tectonics and Paleo-tsunami records of the Northern Coast of Egypt, Ph.D thesis dissertation, University of Strasbourg (France), 429 pp., 2017.

Salamon, A., Rockwell, T., Ward, S. N., Guidoboni, E. & Comastri, A.: Tsunami hazard evaluation of the Eastern Mediterranean: Historical analysis and selected modeling, Bulletin of the Seismological Society America, 97, 705–724, 2007.

Schmidt, J.F.: Studien ueber Erdbeben. 1-136, 316-360, Leipzig, 1879.

Srinivasalu S, Rajeshwara-Rao N, Thangadurai N, Jonathan M P, Roy P D, Rammohan V and Saravanan P., 2009. Characteristics of 2004 tsunami deposits of northern Tamil Nadu coast, India; Boletin de la Sociedad Geologica Mexicana, 61, 111–118, 2009.

Shah-Hosseini, M., Saleem, A., Mahmoud, A. and Morhange, C.: Coastal boulder deposits attesting to large wave impacts on the Mediterranean coast of Egypt, Natural Hazards, 83 (2), 849-865, 2016.

Shaw, B., Ambraseys, N. N., England, P.C., Floyd, M., Gorman, G.J., Higham, T.F.G., Jackson, J., Nocquet, J-M., Pain, C. C., and Piggott, M. D.: Eastern Mediterranean tectonics and tsunami hazard inferred from the AD 365 earthquake, Nature Geoscience, 1 (April), 268–276, 2008.

Shi, S., Dawson, A.G. & Smith, D.E. Coastal sedimentation associated with the December 12th, 1992 tsunami in Flores, Indonesia, Pure and Applied Geophysics, 144, 525-536, 1995.

Soloviev, S.L., Solovieva, O.N., Go, C.N., Kim, K.S., and Shchetnikov, N.A.: Tsunamis in the Mediterranean Sea 2000 B.C.-2000 A.D., Advances in Natural and. Technological Hazards Research, Kluwer Academic Publishers, Dordrecht,. Netherlands, 13, 237 p., 2000.

Stanley, J.D. – Bernasconi, M.P.: Holocene depositional patterns and evolution in Alexandria's eastern harbor, Egypt, Journal of Coastal Research, 22 (2), 283-297, 2006.

Stiros, S. C.: The AD 365 Crete Earthquake and Possible Seismic Clustering During the Fourth to Sixth Centuries AD in the Eastern Mediterranean: A Review of Historical and Archaeological Data, Journal of Structural Geology, 23, 545–562, 2001.

Stiros, S., and Drakos, A.: A fault model for the tsunami-associated magnitude >8.5 Eastern Mediterranean, AD 365 earthquake, Zeitschriftfür Geomorphologie, 146, 125–137, 2006.

Spiske, M., Böcz, Z., and Bahlburg, H.: The role of porosity in discriminating between tsunami and hurricane emplacement of boulders—a case study from the Lesser Antilles, southern Caribbean, Earth Planet. Science Letters, 268, 384–396, 2008.

Switzer, A. D. and Jones, B. G.: Large scale washover sedimentation in a freshwater lagoon from the southeast Australian coast: sea level change, tsunami or exceptionally large storm?, The Holocene, 18 (5), 787-803, 2008.

Szczucinski, W., Chaimanee, N., Niedzielski, P., Rachlewicz, G., Saisuttichai, D., Tepsuwan, T., Lorene, S. and Siepak, J.: Environmental and geological impacts of the 26 December 2004 Tsunami in coastal zone of Thailand- Overveiw of short and long term effects. In: Polish Journal of Environmental studies, 15 (5), 793-810, 2006.

Taymaz, T., Westaway, R., and Reilinger, R.: Active faulting and crustal deformation in the Eastern Mediterranean region, Tectonophysics, 391, 1–9, 2004.

Tinti, S., Maramai, A. and Graziani, L.: A New Version of the European Tsunami Catalogue: Updating and Revision, Natural Hazards and Earth System Sciences, 1, 255-262, 2001.

Tinti, S., Manucci, A., Pagnoni, G., Armigliato, A., and Zaniboni, F.: The 30 December 2002 landslide-induced tsunamis in Stromboli: sequence of the events reconstructed from the eyewitness accounts, Natural Hazards and Earth System Science, 5 (6), 763–775, 2005.

Tuttle, M.P., Ruffman, A., Anderson, T., and Jeter, H.: Distinguishing tsunami from storm deposits in eastern North America: the 1929 Grand Banks tsunami versus the 1991 Halloween storm, Seismological Research letters, 75, 117-31, 2004.

Yalciner, A., Zaytsev, A., Aytore, B., Insel, I., Heidarzadeh, M., Kian, R., and Imamura, F.: A Possible Submarine Landslide and Associated Tsunami at the Northwest Nile Delta, Mediterranean Sea: Oceanography, 27, (2), 68–75, 2014.

Figure captions

Figure1: Seismicity (instrumental with M> 5.5) and main tectonic framework of the east Mediterranean regions. Black boxes indicate the paleoseismic sites of Kefr Saber and El Alamein east of the Nile delta. The major historical earthquakes (Table 1) AD 365 (Mw 8 – 8.5), AD 1303 (Mw ~8) and AD 1870 (Mw ~7.5) are located along the Hellenic subduction zone according to Guidoboni et al. (1994), Stiros (2001); Ambraseys (2009); Papadopoulos et al. (2014) and Jusseret and Sintubin (2017). Focal mechanisms are CMT-Harvard (last accessed January 2018), and the background topography is from GEBCO.

Figure 2: Location of trenches and core sites at (a) Kafr Saber, (b) El Alamein (see also Figure 1), and (c) Dune ridge and a lagoon south of the Mediterranean Sea as a selected site for coring and trenching.

Figure 3: a) Trench dimensions at Kefr Saber, and (b) description of sedimentary layers of trench P 4 with carbon dating sampling (yellow flag); the horizontal ruler indicates 20 cm scale.

Figure 4: Radiocarbon dating calibrated with probability density function (pdf) using Oxcal version 4.2 (Bronk-Ramsey, 2013) and chronology of sedimentary layers and tsunami record of trenches at Kefr Saber. The dating characteristics are in Table 2 a. The Bayesian dating simulation of the white sandy unit in Fig. 3 b can be correlated with the 365 AD tsunami event.

Figure 5: a) Core 1 description with X-ray scanning, lithology log, magnetic susceptibility, mean grain size, sediment sorting, total organic and inorganic matter and bulk mineralogy**.** The arrows show the high values of each measurement that may correlate with tsunami deposits.

b) Core 9 photography, X-ray scanning, lithology log, magnetic susceptibility, mean grain size, sediment sorting, total organic and inorganic matter and bulk mineralogy**.** The arrows show the high values of each measurement that may correlate with tsunami deposits.

(Similar illustrations of cores 2 to 12 are in supplemental materials).

Figure 6: Radiocarbon dating calibrated with probability density function (pdf) using Oxcal version 4.2 (Bronk-Ramsey, 2013) and chronology of sedimentary layers with dated tsunami records at El Alamein. The dating characteristics are in Table 2 b. Black pdfs refer to the dated samples and red pdfs are simulated dating of the four tsunami records. Three sedimentary records are correlated with the historical earthquake and tsunami catalogue of the eastern Mediterranean (See also Table 1).

Figure 7: Depth distribution of tsunami layers in cores at the El Alamein site (see also core locations in Fig. 2 b). The depth correlation of paleotsunami layers indicates the consistent succession of deposits in the lagoon. Deposits of layers 1, 2 and 3 are related with tsunami events 1870 AD, 1303 AD and 365 AD of the East Mediterranean Sea (see also Fig. 6 and Table 1). Layer 4 corresponds to tsunami event 1491 – 1951 BC and is not reported in tsunami catalogues.

Table captions

Table 1: Major earthquakes of the eastern Mediterranean with tsunami wave reports in northern Egypt. Estimated magnitudes are given in Mw when calculated and in M when estimated.

Table 2 a: Radiocarbon dating samples and calibrated ages at Kefr Saber site using OxCal v4.2.4 (Bronk-Ramsey, 2013).

Table 2 b: Radiocarbon dating samples and calibrated ages in El Alamein site using OxCal v4.2.4 (Bronk-Ramsey, 2013)

Table 1: Major earthquakes of the eastern Mediterranean with tsunami wave reports in northern Egypt. Estimated magnitudes are given in Mw when calculated and in M when estimated.

Date	Epicentre	Estimated Magnitude	Comment	Reference
21 July 365	Western Crete	8.3 – 8.5 (M_w)	Tsunami northern Egypt	Stiros and Drakos, 2006; Shaw et al., 2008, Hamouda 2009
18 Jan. 746	Dead Sea Fault	7.5 (M)	Tsunami eastern Medit.	Ambraseys, 1962
881 - 882	Palestine	?	Tsunami in Alexandria & Palestine	Galanopoulos A., 1957
4 Jan. 1033	Jordan Valley Fault	7.4 (M)	Tsunami northern Egypt	Ambraseys, 1962
18 Jan. 1068	Northern Lebanon	6.9 (M)	Waves in Lebanon Until northern Egypt	Ambraseys, 1962, Soloviev et al., 2000
8 Aug. 1303	Karpathos & Rhodos islands	8 (M)	>8-m-high wave in Alexandria	Abu al-Fida1329, Ambraseys 2009, Hamouda 2006
24 June 1870	Hellenic Arc	M_L 7.2	Inundation in Alexandria harbour	Ben-Menahem, 1979, Soloviev et al., 2000

Table 2 a: Radiocarbon dating samples and calibrated age at Kefr Saber site using OxCal v4.2.4 (Bronk-Ramsey, 2013).

No.	**Sample name**	**Laboratory Name**	**Type of samples**	**Depth (m)**	**Date BP**	**Calibrated. date**
1	KSB2S2	Poznan	Dendropoma	Boulder	890 ± 30 BP	940 - 1446 AD
2	TSU P1 S07B	Poznan	Charcoal	35	110.14±0.3 BP	Modern
3	TSU P1 S09B	CIRAM	Charcoal	53	40560 BP	39000-38250 BC
4	TSU P3S2	CIRAM	charcoal	73	2000 BP	50-70 AD
5	TSU P3S3	CIRAM	Charcoal	100	6240 BP	5300 – 5070 BC
6	TSU P3 S2	Poznan	Charcoal	72	1075 ± 30 BP	890 – 1020 AD
7	TSU P4 S2	CIRAM	Charcoal	61	Modern	-
8	TSU P4 S3	CIRAM	Charcoal	40	Modern	-
9	TSU P4 S4	CIRAM	Charcoal	15	Modern	-
10	TSU P4 S5	Poznan	Charcoal	60	15490 ± 70 BP	17200 – 15900 BC
11	TSU P4 S6	Poznan	Charcoal	25	101.42 ± 0.68 BP	1700 – 1920 AD
12	TSU P5S1	Poznan	Charcoal	12	2145 ± 30 BP	360 – 50BC
13	TSU P5S2	Poznan	Charcoal	37	4560 ± 300 BP	4000 – 2400 BC
14	TSU P5S3	Poznan	Charcoal	17	2060 ± 35 BP	180 – 30 AD
15	TSU P5S4	Poznan	Charcoal	33	2590 ± 140 BP	1050 – 350 BC

- CIRAM Lab. science for art cultural heritage ,archeology department http://www.ciram-art.com/en/archaeology.html
- Poznan Lab. Poznan Radiocarbon Laboratory, Poland, email: c.fourteen@radiocarbon.pl http://radiocarbon.pl/index.php?lang=en.
- Beta Analytic radiocarbon dating, Miami, Florida, USA http://www.radiocarbon.com/, e-mail: lab@radiocarbon.com

Table 2 b: Radiocarbon dating samples and calibrated date in El Alamein site using OxCal v4.2.4 (Bronk-Ramsey, 2013)

No.	Sample name	Laboratory Name	Type of samples	Depth (m)	Date BP	Calibrated date (2σ)
a	AL1 S1 (test pit)	CIRAM	charcoal	25	130±20	1680-1908 AD
b	AL1 S2 (test pit)	CIRAM	charcoal	56	190±20	1661-1931 AD
1	core 1/1sa1	Poznan	charcoal	40	13430±60	13985-14415 BC
2	core 1/1sa2	Poznan	Bone	50	1540±60	403-634 AD
3	core2/1sa4	Poznan	gastropods	77	35500±500	34362-36931 BC
4	core2/1sa6	Poznan	gastropods	75	32000±360	32971-34681 BC
5	core 3/1sa1	Poznan	shell	45	33500±600	34218- 37224 BC
6	core 3/1sa2	Poznan	bivalve	37	45000±2000	43618 BC
7	core 4/1sa1	Poznan	shell	28	31840±350	32887-34447BC
9	core 6/2 sa1	Poznan	charcoal	80	125±30	<1620 AD
10	core 6/1 sa6	Poznan	gastropod	45	34000±400	35002-37441 BC
11	core 6/1sa9	Poznan	coral	60	50000±4000	42776-69225 BC
12	core 7/1sa1	Poznan	shell	17	3000±30	293-1113 BC
12	core 9/1sa1	Poznan	gastropod	24	3320±30	1052-1888 BC
13	core 9/1sa5	Poznan	bivalve	55	40000±800	40521-43169 BC
14	core 10/1sa2	Poznan	bone	70	42000±1300	41256-46581 BC
15	core10/1sa3	Poznan	shells	20	4515 ±30	2623-3521 BC
16	core11/2sa1	Beta analytic	roots	139	4810±30	2666 - 2817 BC
17	core 11/1sa1	Beta analytic	gastropod	20	5230±30	3638-4328 BC
18	core11/2Sa4	Poznan	gastropod +shell	116	4500±35	2619-3386 BC
19	core11/2sa6	Poznan	gastropod	126	4405±35	2477-3368 BC
20	core11/2 sa11	Beta analytic	shells	152	32500±500	33294-36120 BC
21	core 11/2sa2	Beta analytic	shell	62	16900±60	17869-18741 BC
22	core 11-2	Beta analytic	charcoal	180	5020±30	3710-3943 BC
23	core 11 2_5	Poznan	gastropod	121	4360±40	2457-3366 BC
24	core 12/1 sa1	Poznan	gastropod	44	5065±30	3367-4072 BC
25	core 12/2sa1	Beta analytic	gastropod	108	4885±35	3097-3950 BC
26	core 12/2sa2	Poznan	gastropod	114	5000±35	3331-4050 BC
27	core 12/2 sa3	Beta analytic	broken shell	117	37940±420	39560 -40811 BC
28	core 12/2sa4	Beta analytic	roots	135	5060±30	3365-4071 BC

- CIRAM Lab. science for art cultural heritage ,archeology department http://www.ciram-art.com/en/archaeology.html

- Poznan Lab. Poznan Radiocarbon Laboratory, Poland, email: c.fourteen@radiocarbon.pl http://radiocarbon.pl/index.php?lang=en.
- Beta Analytic radiocarbon dating, Miami, Florida, USA http://www.radiocarbon.com/, e-mail: lab@radiocarbon.com

Figure 1

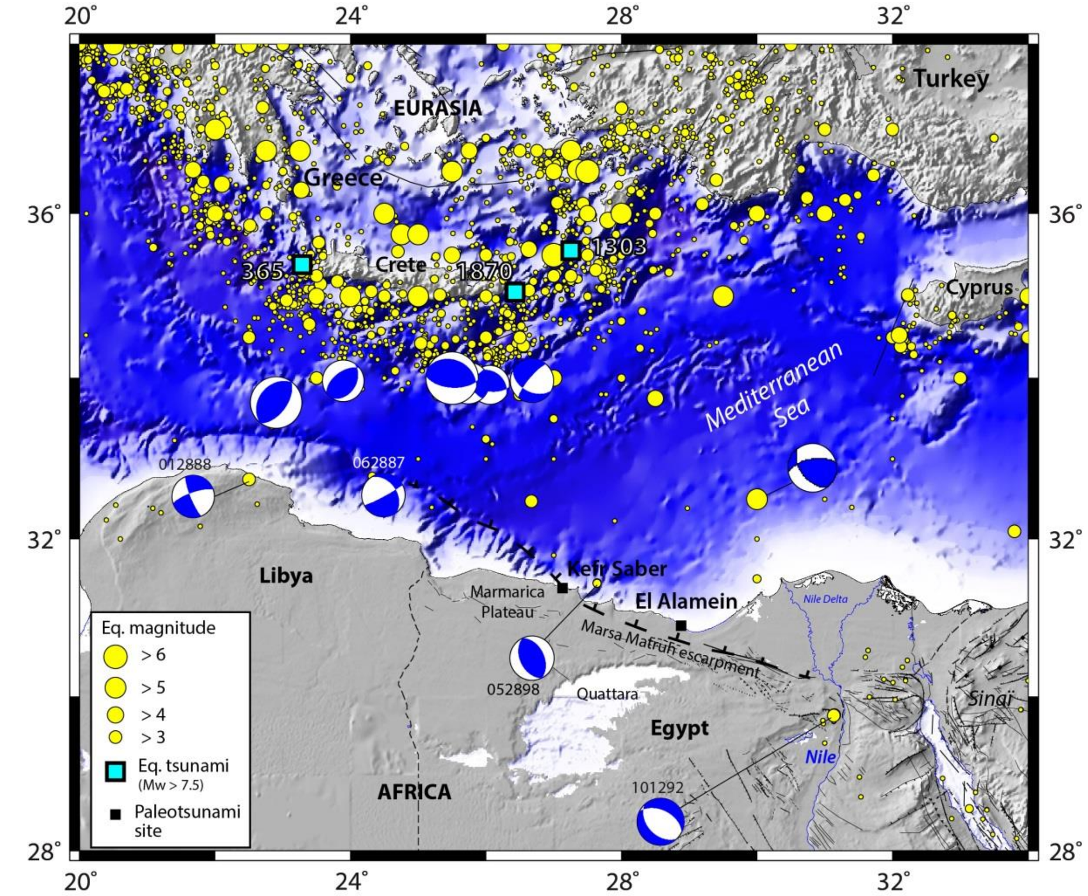
20°
24°
28°
32°
36°
EURASIA
Turkey
Greece
365
Crete
1870
1303
Cyprus
Mediterranean Sea
012888
062887
Libya
Kefr Saber
Marmarica Plateau
El Alamein
Nile Delta
Marsa Matruh escarpment
052898
Quattara
Egypt
Sinai
Nile
AFRICA
101292
Eq. magnitude
> 6
> 5
> 4
> 3
Eq. tsunami (Mw > 7.5)
Paleotsunami site

Figure 2

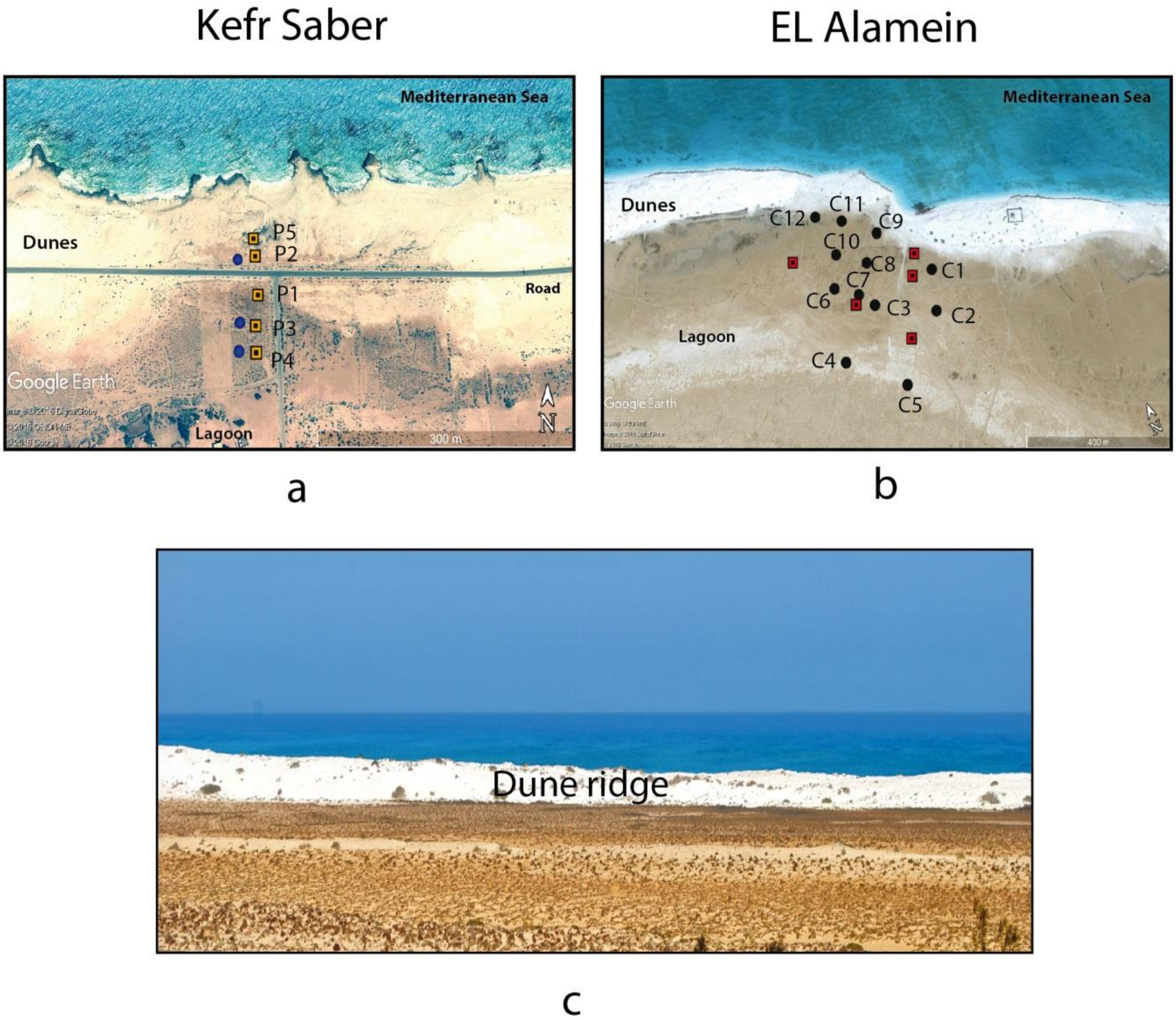
Kefr Saber
EL Alamein
Mediterranean Sea
Dunes
P5
P2
P1
P3
P4
Road
Lagoon
Google Earth
300 m
Mediterranean Sea
Dunes
C12
C11
C9
C10
C8
C1
C7
C6
C3
C2
Lagoon
C4
C5
Google Earth
400 m
a
b
Dune ridge
c

Figure 3

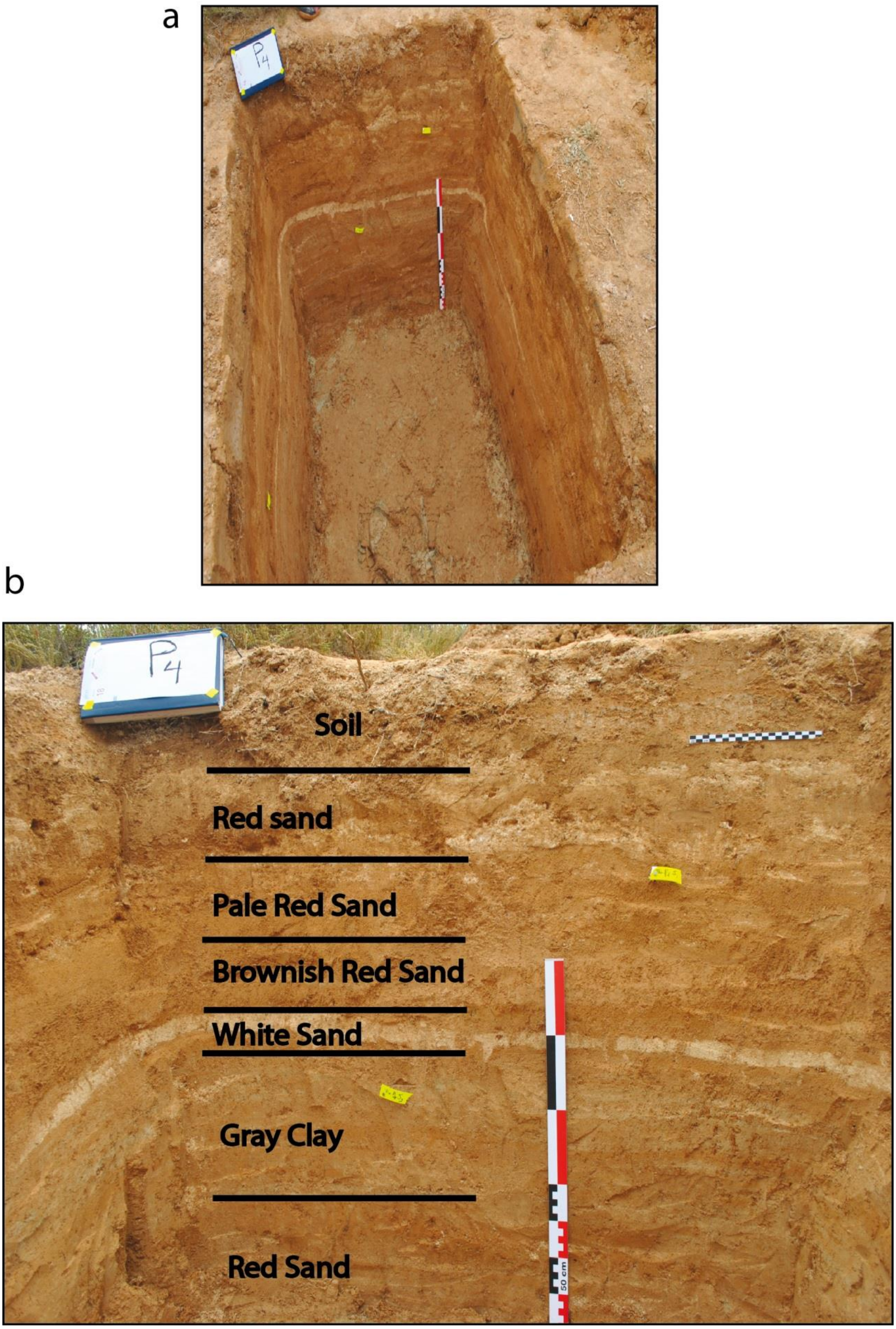
a
P4
b
P4
Soil
Red sand
Pale Red Sand
Brownish Red Sand
White Sand
Gray Clay
Red Sand
50 cm

Figure 4

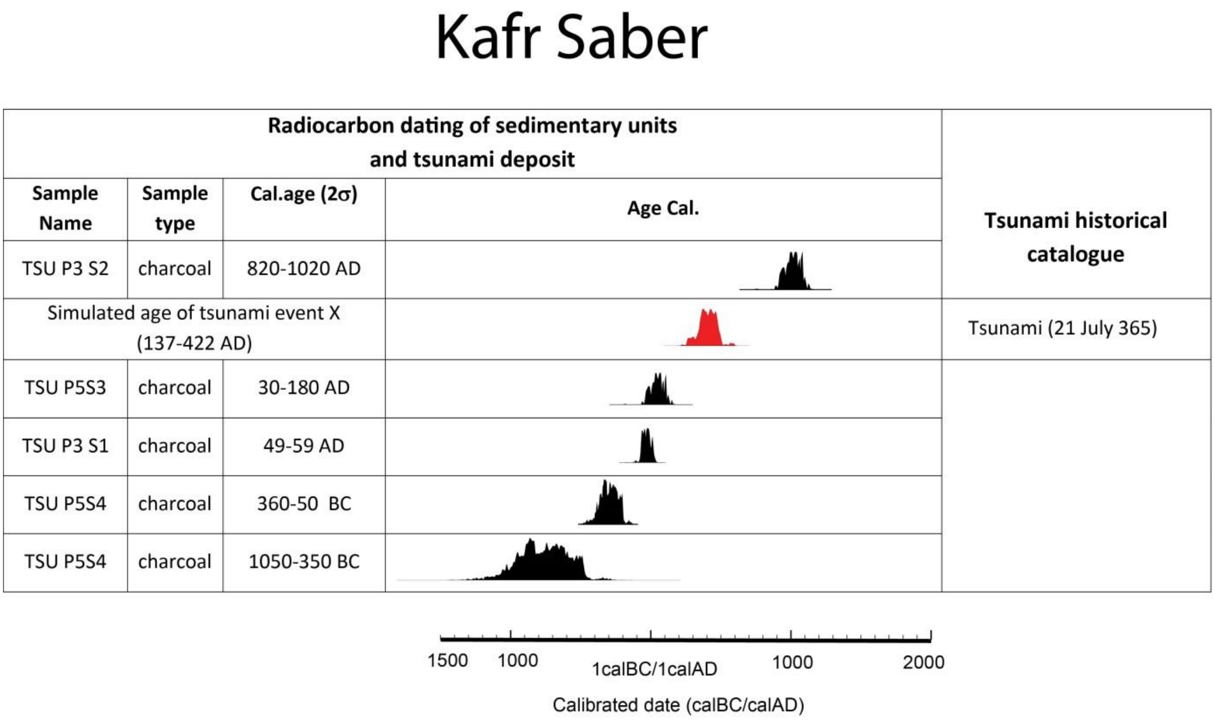

Radiocarbon dating of sedimentary units and tsunami deposit				Tsunami historical catalogue
Sample Name	Sample type	Cal.age (2σ)	Age Cal.	
TSU P3 S2	charcoal	820-1020 AD		
Simulated age of tsunami event X (137-422 AD)				Tsunami (21 July 365)
TSU P5S3	charcoal	30-180 AD		
TSU P3 S1	charcoal	49-59 AD		
TSU P5S4	charcoal	360-50 BC		
TSU P5S4	charcoal	1050-350 BC		

Figure 5 a

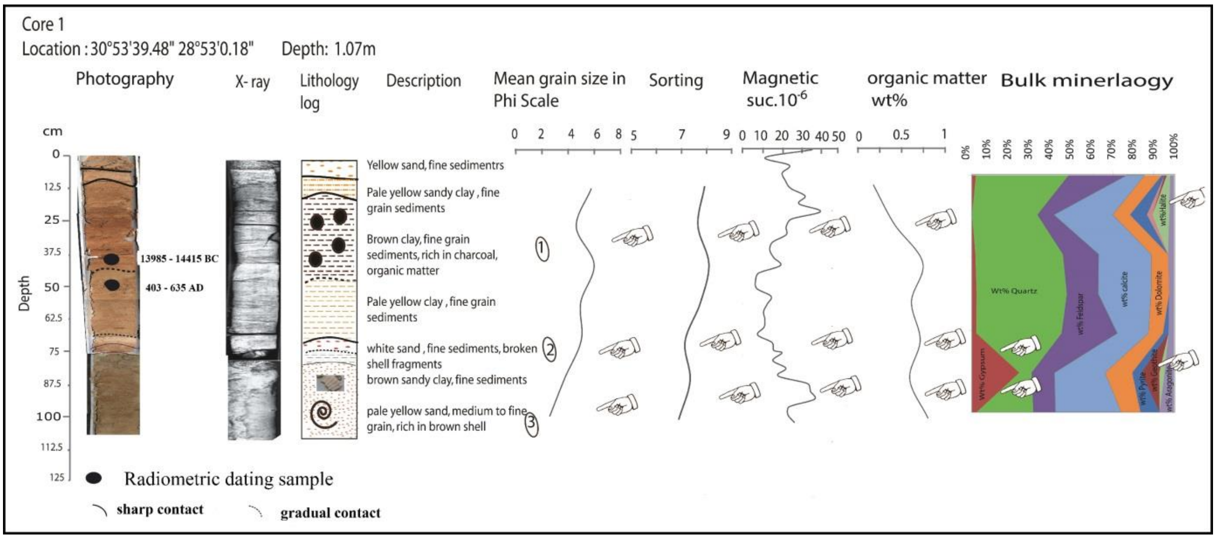

Figure 5 b

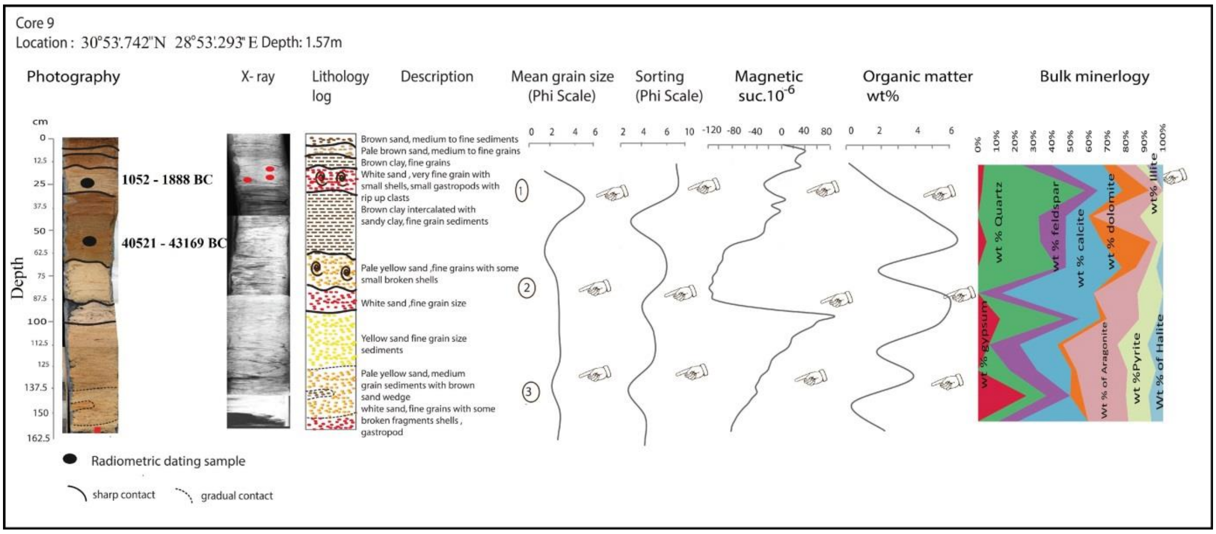

Figure 6

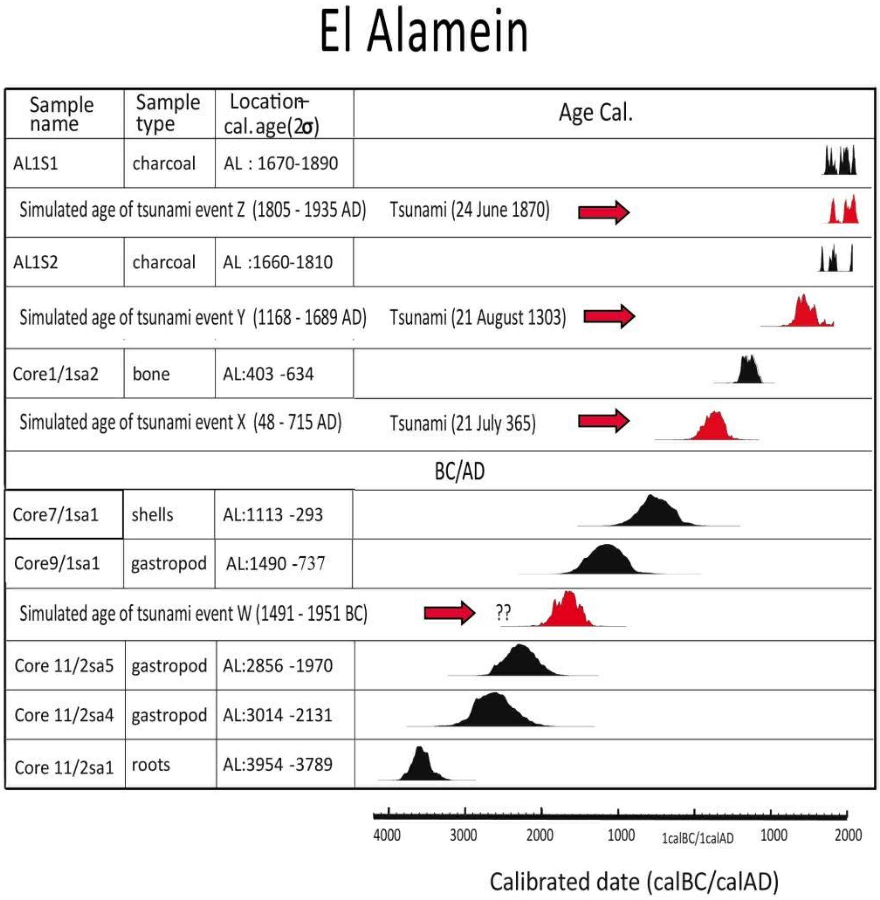

Figure 7

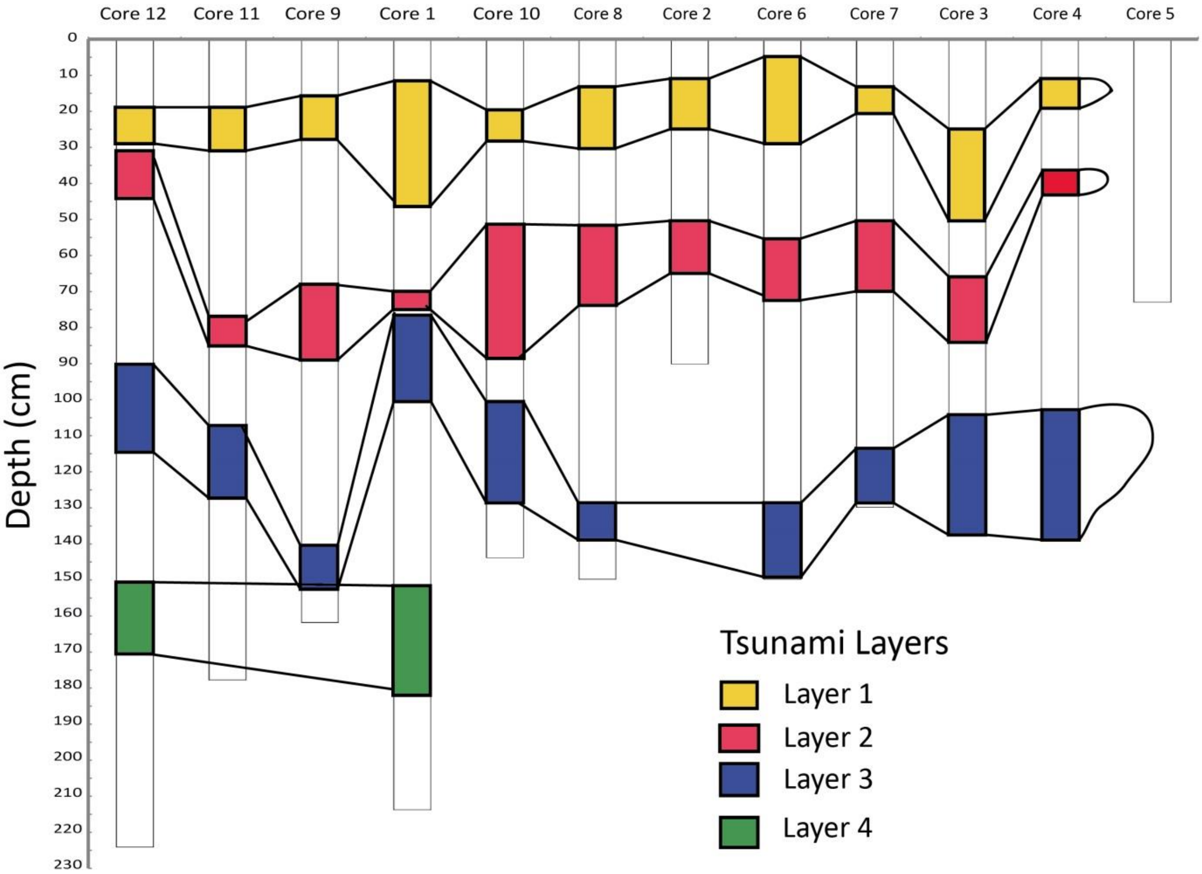
Core 12
Core 11
Core 9
Core 1
Core 10
Core 8
Core 2
Core 6
Core 7
Core 3
Core 4
Core 5
Depth (cm)
0
10
20
30
40
50
60
70
80
90
100
110
120
130
140
150
160
170
180
190
200
210
220
230
Tsunami Layers
Layer 1
Layer 2
Layer 3
Layer 4